

# Intrinsic neutron background of nuclear emulsions for directional Dark Matter searches

A. Alexandrov<sup>a</sup>, T. Asada<sup>b</sup>, A. Buonaura<sup>a,c</sup>, L. Consiglio<sup>d</sup>, N. D'Ambrosio<sup>d</sup>, G. De Lellis<sup>a,c</sup>, A. Di Crescenzo<sup>a</sup>, N. Di Marco<sup>d</sup>, M. L. Di Vacri<sup>d</sup>, S. Furuya<sup>b</sup>, G. Galati<sup>a,c</sup>, V. Gentile<sup>a,c</sup>, T. Katsuragawa<sup>b</sup>, M. Laubenstein<sup>d</sup>, A. Lauria<sup>a,c</sup>, P. F. Loverre<sup>e,f</sup>, S. Machii<sup>b</sup>, P. Monacelli<sup>e</sup>, M. C. Montesi<sup>a,c</sup>, T. Naka<sup>b</sup>, F. Pupilli<sup>g,\*</sup>, G. Rosa<sup>e,f</sup>, O. Sato<sup>b</sup>, P. Strolin<sup>a,c</sup>, V. Tioukov<sup>a</sup>, A. Umemoto<sup>b</sup>, M. Yoshimoto<sup>b</sup>

<sup>a</sup>INFN Sezione di Napoli, I-80125 Napoli, Italy

<sup>b</sup>Nagoya University, J-464-8602 Nagoya, Japan

<sup>c</sup>Dipartimento di Fisica dell'Università Federico II di Napoli, I-80125 Napoli, Italy

<sup>d</sup>INFN - Laboratori Nazionali del Gran Sasso, I-67010 Assergi (L'Aquila), Italy

<sup>e</sup>INFN Sezione di Roma, I-00185 Roma, Italy

<sup>f</sup>Dipartimento di Fisica dell'Università di Roma Sapienza, I-00185 Roma, Italy

<sup>g</sup>INFN - Laboratori Nazionali di Frascati dell'INFN, I-00044 Frascati (Roma), Italy

## Abstract

Recent developments of the nuclear emulsion technology led to the production of films with nanometric silver halide grains suitable to track low energy nuclear recoils with submicrometric length. This improvement opens the way to a directional Dark Matter detection, thus providing an innovative and complementary approach to the on-going WIMP searches. An important background source for these searches is represented by neutron-induced nuclear recoils that can mimic the WIMP signal. In this paper we provide an estimation of the contribution to this background from the intrinsic radioactive contamination of nuclear emulsions. We also report the neutron-induced background as a function of the read-out threshold, by using a GEANT4 simulation of the nuclear emulsion, showing that it amounts to about 0.06 per year per kilogram, fully compatible with the design of a 10 kg  $\times$  year exposure.

## Keywords:

Dark matter, Neutron background, Radiopurity, Nuclear emulsions

## 1. Introduction

There is a compelling evidence [1], mostly coming from astrophysical observations [2], for the existence of Dark Matter in the Universe. Many direct search experiments are testing the WIMP (Weakly Interactive Massive Particle) hypothesis as Dark Matter candidate by measuring the energy transferred to target nuclei through the WIMP-nucleus scattering. They look for an excess of events over the expected background or for annually modulated signals [3] but they lead to controversial results: the annually modulated signal observed by DAMA/LIBRA [4] is in tension with upper limits on the interaction cross section reported by other experiments [5, 6, 7, 8, 9].

An unambiguous signature of WIMPs would come from the observation of a non-isotropic signal with respect to the isotropically distributed background: indeed, due to the relative motion of the solar system with respect to the galactic halo, the WIMP flux should mostly come from the direction of this motion (i.e. from the Cygnus constellation) and nuclear recoils induced by WIMPs should show a peak in the opposite direction [10]. Recoil tracks in solid targets are expected to be in the sub- $\mu\text{m}$  range and require an unprecedented spatial accuracy. Therefore many efforts have been pursued exploiting low-pressure gas detectors, like DRIFT [11], NEWAGE [12],

DMTPC [13], MIMAC [14]; nevertheless these approaches require large target volumes in order to be sensitive to low WIMP spin-independent interaction cross sections, and the small mass exposures performed so far are limited by non-trivial scalability problems.

A recent proposal [15, 16] foresees the use of nuclear emulsions both as target and as tracking device for a WIMP directional search. Nuclear emulsion consists of a large number of sensitive silver bromide crystals, usually with linear dimensions of about 200 nm, like the one used for OPERA films [17], dispersed in an organic gelatin matrix, composed essentially by hydrogen, carbon, nitrogen and oxygen. Through-going ionizing particles release energy to the crystals creating sensitised sites along their trajectories, the latent image. By the action of a mild chemical reducing agent, a photographic developer, the conversion of halide to metallic silver selectively affects sensitised crystals. After the development, followed by fixing and washing, the gelatin becomes optically transparent. Three-dimensional paths of charged particles are finally visible as trails of silver grains using optical microscopes.

The production of films with a crystal diameter of  $40\pm 9$  nm and a linear density of 11 crystals/ $\mu\text{m}$  was achieved for the first time in 2007 [18]. Further upgrades [19] have produced samples with a linear dimension of  $18\pm 5$  nm, one order of magnitude smaller than OPERA films [17]; their linear density is  $\sim 29$  crystals/ $\mu\text{m}$ , implying an intrinsic detector threshold of about 50 nm, if we consider tracks of at least two grains. This

\*Corresponding author

Email address: fabio.pupilli@lnf.infn.it (F. Pupilli)

threshold corresponds to a recoil energy of carbon (silver) nuclei of about 20 keV (110 KeV).

Radiogenic backgrounds have to be reduced and taken under control when dealing with signals as rare as the WIMP-nucleon scattering.

The energy deposition per unit path length of WIMP-induced recoils is expected to be, for light and heavy nuclei respectively, one or two orders of magnitude larger than the one due to electrons [20]; therefore  $\gamma$ -rays and  $\beta$ -particles can be rejected by properly controlling the emulsion response, in terms of number of sensitised crystals per unit path length (*sensitivity*), through the chemical treatment of the emulsion itself.

$\alpha$ -particles, essentially coming from Uranium and Thorium decay chains, have energies of the order of MeV and can therefore be identified by their 3D range and rejected by an upper cut on the track length. For this purpose, a tomographic emulsion scanning with micrometric resolution, like the one performed in OPERA [21] and able to reconstruct also perpendicular tracks, will be performed.

The most important background is represented by neutrons since they induce nuclear recoils with track lengths comparable to the WIMP-induced ones. For external sources we plan to inherit and adapt passive shielding strategies successfully implemented in other dark matter experiments and to operate the detector underground, for the reduction of the cosmogenic contribution. Intrinsic contamination of nuclear emulsions by Uranium and Thorium traces is responsible for an irreducible neutron yield through ( $\alpha,n$ ) reactions and  $^{238}\text{U}$  spontaneous fission. This neutron source is unavoidable and can be minimized only by a proper selection and/or pre-treatment of the emulsion components. The aim of this publication is to set the scale of this irreducible background contribution.

After a description of the constituents and of the elemental composition of nuclear emulsions we report the measurements of the intrinsic radioactive contamination. We then derive the related neutron yield and its energy spectrum. Based on a GEANT4 [22] simulation of nuclear emulsions, we estimate the intrinsic background induced by neutrons. We finally conclude that, even without a dedicated selection of the emulsion components, it is compatible with an emulsion exposure of  $O(10)$  kg  $\times$  year.

## 2. Nuclear emulsion composition and intrinsic radioactive contamination

Nuclear emulsions are composed by an organic gelatin matrix acting as retaining structure for their sensitive elements, the silver bromide crystals. The emulsions developed for directional Dark Matter searches consist of a larger fraction of AgBr crystals with smaller dimension with respect to the standard ones; crystals are also doped with iodine to increase their sensitivity to ionizing particles. It should be mentioned that the presence of iodine slightly enhance the detector sensitivity to spin-dependent WIMP interactions. Polyvinyl alcohol (PVA) is used to stabilise and reduce the crystal growth. AgBr-I crystals are uniformly dispersed in a homogeneous mixture

of gelatin and PVA. The results reported hereafter are based on samples provided by the Nitta Gelatin (cow's bones gelatin), the Kanto-Kagaku for AgBr and the Sigma-Aldrich for the PVA. The mass fractions of the emulsion constituents are reported in Table 1a, while in Table 1b the elemental composition is detailed. The emulsion composition, key ingredient for the neutron yield estimation and for the GEANT4 simulation, has been carefully determined for light elements by an elemental analyser (YANACO MT-6); their measurements were performed with a relative humidity ranging from 30% to 40% and have an absolute uncertainty of 0.003. We have measured that a 10% variation in relative humidity induces changes in H and O mass fractions well within this uncertainty. The mass fraction of silver and bromine has been measured by an energy dispersive X-ray analysis with an absolute uncertainty of 0.02. The density amounts to  $3.43 \text{ g cm}^{-3}$ .

Constituent	Mass Fraction
AgBr-I	0.78
Gelatin	0.17
PVA	0.05

(a) Constituents of nuclear emulsion

Element	Mass Fraction	Atomic Fraction
Ag	0.44	0.10
Br	0.32	0.10
I	0.019	0.004
C	0.101	0.214
O	0.074	0.118
N	0.027	0.049
H	0.016	0.410
S	0.003	0.003

(b) Elemental composition

Table 1: Composition of the nuclear emulsion. The uncertainties on mass fractions are reported in the text.

A sample of each component of the nuclear emulsion has been analysed by the Chemistry Service in Laboratori Nazionali del Gran Sasso (LNGS, Italy), with the Inductively Coupled Plasma Mass Spectrometry (ICP-MS) technique [23], in order to determine the Uranium and Thorium contamination; the instrument used for the analysis is a 7500a model from Agilent Technologies and the results obtained have an uncertainty of 30%. The measured contaminations are reported in Table 2 for all the constituents, together with the corresponding activities obtained through the conversion factors  $1 \text{ Bq kg}^{-1}$  ( $^{238}\text{U}$ )  $\equiv 81 \times 10^{-9} \text{ g g}^{-1}$  ( $^{238}\text{U}$ ),  $1 \text{ Bq kg}^{-1}$  ( $^{232}\text{Th}$ )  $\equiv 246 \times 10^{-9} \text{ g g}^{-1}$  ( $^{232}\text{Th}$ ) [24]. The upper limits on PVA are evaluated at 95% CL.

By weighting the measured activity of each constituent for its mass fraction, the total activity of nuclear emulsion can be calculated; for PVA we assume conservatively a 95% CL upper limit. The  $^{238}\text{U}$  activity amounts to  $23 \pm 7 \text{ mBq kg}^{-1}$  (i.e.  $(1.9 \pm 0.6) \times 10^{-9} \text{ g g}^{-1}$ ), while the  $^{232}\text{Th}$  one is  $5.1 \pm 1.5 \text{ mBq kg}^{-1}$  (i.e.  $(1.3 \pm 0.4) \times 10^{-9} \text{ g g}^{-1}$ ). The reported errors are

Nuclide	Contamination [ $10^{-9} \text{ g g}^{-1}$ ]	Activity [ $\text{mBq kg}^{-1}$ ]
AgBr-I		
$^{232}\text{Th}$	1.0	4.1
$^{238}\text{U}$	1.5	18.5
Gelatin		
$^{232}\text{Th}$	2.7	11.0
$^{238}\text{U}$	3.9	48.1
PVA		
$^{232}\text{Th}$	< 0.5	< 2.0
$^{238}\text{U}$	< 0.7	< 8.6

Table 2: Results obtained by ICP-MS in terms of contamination and activity for the different constituents of the nuclear emulsion. The estimated uncertainty is 30%. The upper limits on PVA are evaluated at 95% CL.

Decay chain	Nuclide	Contamination [ $10^{-9} \text{ g g}^{-1}$ ]	Activity [ $\text{mBq kg}^{-1}$ ]
AgBr-I			
$^{232}\text{Th}$	$^{228}\text{Ra}$	< 2.9	< 12
	$^{228}\text{Th}$	< 1.4	< 5.5
$^{238}\text{U}$	$^{226}\text{Ra}$	< 0.7	< 8.9
	$^{234}\text{Th}$	< 18	< 220
Gelatin			
$^{232}\text{Th}$	$^{228}\text{Ra}$	< 0.3	< 1.3
	$^{228}\text{Th}$	$5.0 \pm 0.4$	$20 \pm 2$
$^{238}\text{U}$	$^{226}\text{Ra}$	$0.19 \pm 0.05$	$2.4 \pm 0.6$
	$^{234}\text{Th}$	< 6.4	< 79

Table 3: Results obtained by  $\gamma$ -spectroscopy in terms of contamination and activity for the different constituents of the nuclear emulsion. The upper limits are evaluated at 90% CL.

dominated by the 30% uncertainty in the radioactive contamination measurements. By assuming a null contribution from PVA, the previous contaminations are reduced by  $\sim 2\%$ .

In nature Uranium and Thorium decay chains are found in secular equilibrium; therefore, in order to calculate the neutron yield from  $(\alpha, n)$  reactions, the same activity of the parent is assumed for all the daughter nuclides in the chain. Nevertheless, the human intervention during the manufacturing process may alter the equilibrium by artificially modifying the quantity of some nuclides in the chain. In order to verify the validity of this assumption and also to cross check the measured activities, the samples were analysed with the  $\gamma$ -spectroscopy technique sensitive to  $\gamma$ -active daughter nuclides. The measurements have been performed in the low background facility STELLA (Sub-Terranean Low Level Assay) of the LNGS [25] with germanium detectors; a sample of about 300 g of AgBr-I and one of about 500 g of gelatin were used and the data taking lasted for about 2 and 3 weeks respectively.

As reported in Table 3, the results for the AgBr-I are in fair agreement with the mass spectrometry measurement and there is no indication for broken decay chains. For the gelatin, the measurements gave comparable results for the  $^{232}\text{Th}$  chain, while the  $\gamma$ -spectroscopy measured a concentration of  $^{226}\text{Ra}$  in

the  $^{238}\text{U}$  chain about 20 times smaller than the parent isotope, with a measured value of  $2.4 \pm 0.6 \text{ mBq kg}^{-1}$ . This measurement suggests a break in the secular equilibrium of the decay chain at this point. For the gelatin, secular equilibrium is assumed for the upper part of the  $^{238}\text{U}$  chain, using the activity measured by mass spectrometry, while, for the lower part, nuclides will be considered in equilibrium with  $^{226}\text{Ra}$  and the activity measured with  $\gamma$ -spectroscopy will be used. Therefore the nuclear emulsion activity for nuclides of the  $^{226}\text{Ra}$  sub-chain, including also the activities of AgBr-I and PVA weighted by the corresponding mass fraction, is  $15 \pm 5 \text{ mBq kg}^{-1}$ .

### 3. Radiogenic neutron yield estimation

The total emulsion activities derived in the previous section are essential to determine the intrinsic neutron yield; indeed Uranium and Thorium decay chains are responsible of neutron generation from detector materials through spontaneous fission and  $(\alpha, n)$  interactions.

Many nuclides undergo spontaneous fission, but the only relevant contribution comes from  $^{238}\text{U}$ , since the number of fissions per decay of other natural elements is at least two orders of magnitude lower. The neutron production rate  $R$  is calculated

Process	SOURCES simulation [kg <sup>-1</sup> y <sup>-1</sup> ]	Semi-analytical calculation [kg <sup>-1</sup> y <sup>-1</sup> ]
( $\alpha$ , n) from <sup>232</sup> Th chain	0.12±0.04	0.11±0.03
( $\alpha$ , n) from <sup>238</sup> U chain	0.27±0.09	0.26±0.08
Spontaneous fission	0.8±0.3	0.8±0.3
Total flux	1.2±0.4	1.2±0.4

Table 4: Neutrons per kilogram per year due to ( $\alpha$ , n) and spontaneous fission reactions in the nuclear emulsion, evaluated with the SOURCES code and semi-analytical calculation.

as:

$$R_{sf} = A \times \psi \times n \quad (1)$$

where  $A$  is the <sup>238</sup>U trace activity,  $\psi = 5.45 \times 10^{-7}$  [26] is the fission probability per decay and  $n = 2.07$  [26] is the average number of neutrons emitted per fission.

The rate from ( $\alpha$ ,n) reactions depends on the rate and energy of  $\alpha$  decays and on the materials in which the radioactive contaminations are embedded. It can be determined with a semi-analytical approach exploiting the experimental neutron yield from different elements and the method reported in reference [27]; this approach relies on the conservative assumption that the nuclear emulsion film is thick enough to let all  $\alpha$  particles to stop or interact inside; if this condition is not satisfied, the calculated neutron flux has to be considered as an overestimation. It is also assumed that ( $\alpha$ ,n) reactions on high  $Z$  elements, such as Ag and Br, do not contribute to the total neutron flux; indeed for these elements the Coulomb barrier of electrons surrounding the nucleus is of the same order of the highest  $\alpha$  energies from natural radioactive chains, and therefore the cross section of the reaction is highly suppressed. The neutron rate is given by:

$$R_{(\alpha,n)} = \sum_i B_i \times y_i^c \quad (2)$$

where  $i$  runs over the  $\alpha$ -emitting nuclides in the Uranium and Thorium chains;  $B_i$  is the total emulsion activity for the  $i$ -th nuclide, as determined in the previous section;  $y_i^c$  is the neutron yield of the whole nuclear emulsion, that can be written in terms of the individual elements as:

$$y_i^c = \sum_j \frac{w_j S_j^m(E_i)}{S_c^m(E_i)} y_{i,j}(E_i) \zeta_i \quad (3)$$

where  $j$  runs over all the elements of the nuclear emulsion;  $w_j$  is the mass fraction of the  $j$ -th element (Table 1b);  $y_{i,j}(E_i)$  is the neutron yield of the  $j$ -th element for an  $\alpha$  particle at energy  $E_i$  emitted by the  $i$ -th nuclide, as derived from [27];  $\zeta_i$  is the branching ratio of the  $i$ -th nuclide decay.  $S_c^m(E_i)$  is the total mass stopping power of the nuclear emulsion at the given energy and, assuming the Bragg additivity rule, it is evaluated as the weighted sum of the mass stopping powers of its elements:

$$S_c^m(E) = \sum_j w_j S_j^m(E) \quad (4)$$

where  $S_j^m$  is given by the stopping power divided by the density  $\rho_j$  of the  $j$ -th element .

The mass stopping powers of each element were taken from the ASTAR database [28]; since bromine is not included in the database, the stopping power values were calculated through the Bethe's formula, using for the mean excitation potential the following empirical formula [29]:

$$I(eV) = (9.76 + 58.8Z^{-1.19})Z \quad (5)$$

with  $Z = 35$ . For the bromine density the value  $3.1028 \text{ g cm}^{-3}$  was used.

In order to cross check the estimation obtained with this approach and to calculate also the neutron spectrum, the SOURCES code [30] was used. The inputs used are the atomic fractions reported in Table 1b, the number of atoms for each  $\alpha$ -emitting nuclide, derived from the activities reported in the previous section, and the atomic fractions of target nuclides, accounting for the natural isotopic abundances [31] of each element.

In the calculation,  $\alpha$ -emitters are assumed to be uniformly distributed in the material. Furthermore, as for the semi-analytical calculation, the thick-target assumption is used and high  $Z$  elements are not considered as target nuclides.

The original version of SOURCES describes ( $\alpha$ ,n) reactions only up to 6.5 MeV  $\alpha$ -energies. This would limit the reliability of the results, both in terms of estimated neutron flux and spectrum, since the reaction cross section and the average neutron energy both increase with the incident  $\alpha$  energy. To overcome this limitation, a modified version of SOURCES [32], able to deal with  $\alpha$ -energies up to 10 MeV, was used.

The neutron production rates from spontaneous fission and ( $\alpha$ ,n) reactions, as determined with both the semi-analytical calculation and the SOURCES code, are reported in Table 4. Following the approach reported in reference [27], we have estimated an uncertainty on  $y_c$  (Eq. 3) of about 9% due to the mass stopping powers, the emulsion composition and the neutron yields of each element. The total uncertainty on the neutron production rate (Eq. 2) is therefore dominated by the 30% contribution due to the activity of  $\alpha$ -decaying nuclides. The SOURCES code uncertainty of 17% quoted in reference [30], convoluted with the 30% uncertainty in the activity estimation, gives a total uncertainty for this computation of 34%.

The two approaches give comparable results and the flux due to the intrinsic radioactive contamination is expected to be of

the order of 1 neutron per year per kilogram of nuclear emulsion. It is worth noticing that the effect of the reduced activity measured with the  $\gamma$ -spectroscopy for the  $^{226}\text{Ra}$  sub-chain of gelatin amounts to less than 10% in the total neutron flux per year per kilogram.

The energy spectrum of the produced neutrons, as calculated with SOURCES, is reported in Figure 1; it is peaked at 0.7 MeV, with a mean value of about 2 MeV.

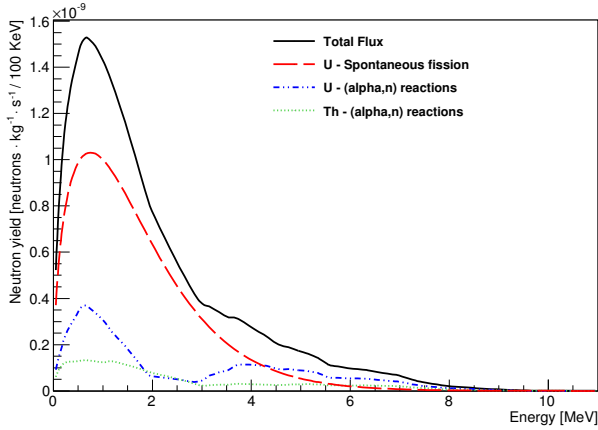


Figure 1: Total neutron energy spectrum (solid black line); in dashed red the contribution from  $^{238}\text{U}$  spontaneous fission is shown, while in dot-dashed blue and dotted green the contributions from  $(\alpha,n)$  reactions due to nuclides in the  $^{238}\text{U}$  and  $^{232}\text{Th}$  chains respectively are displayed.

#### 4. Background estimation

In order to estimate the detectable background due to radiogenic neutrons produced by the intrinsic radioactive contamination of the nuclear emulsions, a GEANT4 [22] based simulation was performed. In the simulated setup two  $50\ \mu\text{m}$  thick nuclear emulsion layers are coated on both sides of a  $175\ \mu\text{m}$  thick plastic base made of Polyethylene terephthalate (PET). This double coated emulsion film is sketched in Figure 2. With the ICP-MS technique, an upper limit of  $20 \times 10^{-12}\ \text{g g}^{-1}$  at 95% CL for both Uranium and Thorium was measured for the PET intrinsic contamination. The resulting upper limit on the neutron flux, estimated with the same approach explained in the previous section, is 60 times lower than the contribution from nuclear emulsion, and therefore is neglected.

1 kg of nuclear emulsion with the same chemical composition described in Table 1b has been simulated.

The fraction of interacting neutrons depends on the ratio between the volume and the surface of nuclear emulsion. For a quantitative estimate, in this work we assume that 50 double coated emulsion films, with a surface of  $25 \times 25\ \text{cm}^2$ , are piled-up for a total thickness of 13.75 mm, corresponding to an emulsion thickness of 5 mm.

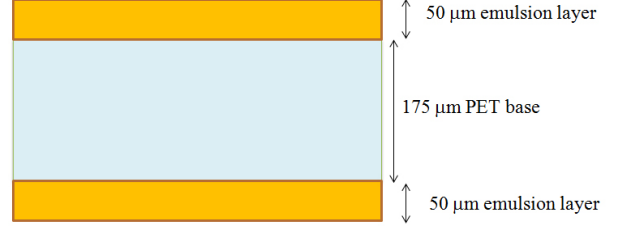


Figure 2: Double coated emulsion film.

One million neutrons were generated with an isotropic angular distribution; they were uniformly distributed in the emulsion material only, given the negligible contribution of the plastic base to the neutron flux. The energy spectrum was generated according to Figure 1. The relevant processes in this energy range are the elastic scattering, the inelastic scattering and the neutron capture. 73.8% of neutrons undergoes at least one interaction, while 36.8% are involved also in secondary interactions. About 65% of neutron interactions happen in PET. Table 5 shows the fractions of different interaction processes, while the fractions of recoiled particles are reported in Table 6.

Process	Fraction
elastic scattering	0.973
inelastic scattering	0.023
neutron-capture	0.004

Table 5: Interaction processes and their fractions.

Recoils	Fraction
nuclei	0.394
protons	0.605
$\alpha$ -particles	0.001

Table 6: Recoiled particles and their fractions.

In order to estimate the background contribution to the proposed Dark Matter search, we have evaluated the track length of the induced recoils. Figure 3 reports the visible track length distribution of proton recoils, defined as the distance between the first and last hit when they both happen in the active emulsion layers. This length ranges from a few nm to several hundreds  $\mu\text{m}$ . The proton energy distribution is also displayed.

Nuclear recoils have a softer spectrum and therefore they exhibit a shorter visible track length, not exceeding  $3\ \mu\text{m}$  for light nuclei (C,N,O,S) and  $1\ \mu\text{m}$  for heavy nuclei (Ag,Br,I), as shown in Figure 4.

The threshold on detectable track lengths in nuclear emulsion depends on the read-out technology: fully automated optical microscopes have shown a good detection efficiency above 200 nm [16]; on-going R&D activities envisage to lower the detectable track length down to the intrinsic detector threshold

	WIMP mass (GeV)		
	10	100	1000
Recoil nucleus	Maximum recoil length (nm)		
C	100	350	430
Ag	11	140	480

Table 7: Maximum WIMP-induced recoil length of Carbon and Silver nuclei for three different WIMP masses.

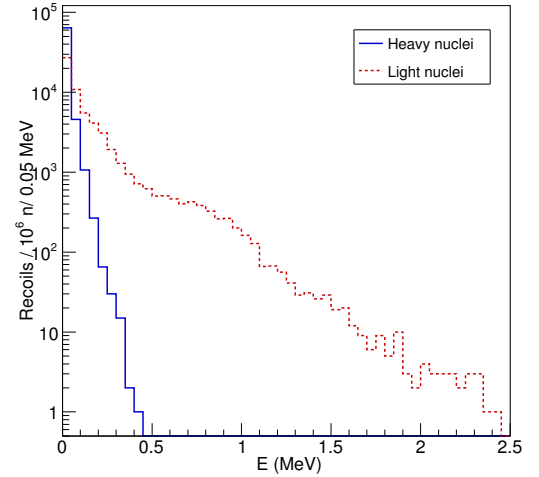
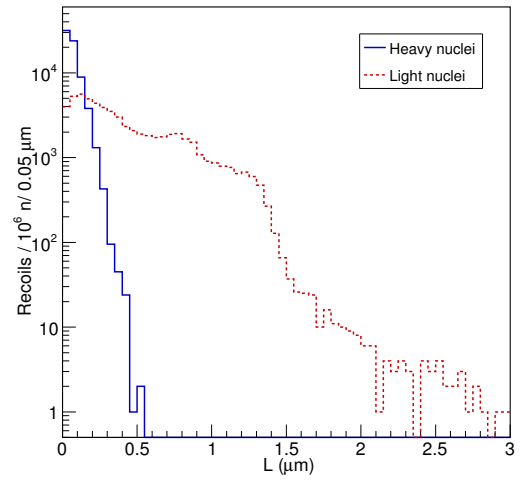
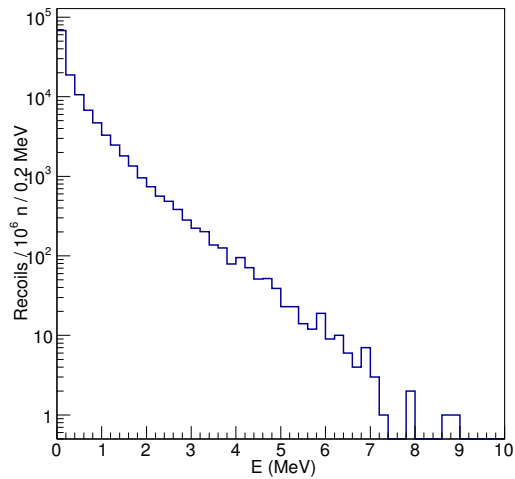
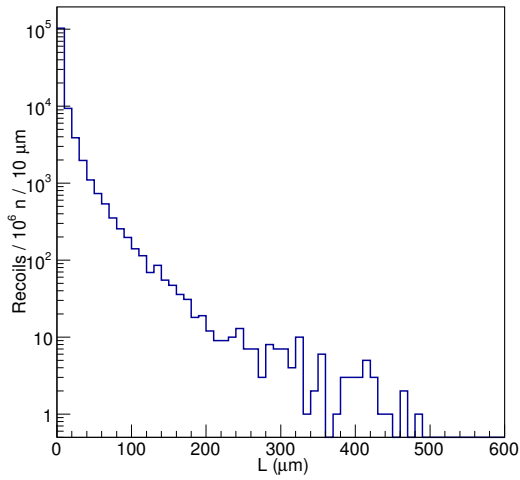


Figure 3: Visible track length (top) and energy spectrum (bottom) for proton recoils.

Figure 4: Visible track length (top) and energy spectrum (bottom) for heavy nuclei (Ag,Br,I) (solid blue line) and light nuclei (C,N,O,S) (dashed red line).

of about 50 nm. We consider in this analysis different detector thresholds between 50 and 200 nm. On the other side an upper limit of 1  $\mu\text{m}$  on the track length can be introduced to suppress the background from radiogenic  $\alpha$  particles, since the signal is expected below 1  $\mu\text{m}$  even for large ( $O(\text{TeV})$ ) WIMP masses, as shown in Table 7. This cut is effective in suppressing also the neutron-induced proton recoils. The fractions of neutron-induced recoils below this cut, as a function of the read-out threshold, are reported in Table 8: only 7% to 14% of the intrinsic neutron flux contributes to the background.

Threshold [nm]	Fraction
50	0.138
100	0.104
150	0.086
200	0.073

Table 8: Fraction of detectable neutron-induced recoils as a function of the read-out threshold, with an upper cut on the track length of 1  $\mu\text{m}$ .

A further background suppression can be obtained by exploiting the directionality information: indeed, as previously stated, the signal produced by WIMP-induced nuclear recoils is expected to have a directional signature. We assume that the surface of the nuclear emulsion will be placed in parallel to the Sun direction in the Galaxy, thanks to an equatorial telescope. In this reference frame, the longitudinal component of the scattering angle is dominant on average and its projection  $\phi$  on the plane of the emulsion surface can be defined. A further reduction of  $\sim 36\%$  of the neutron-induced background can be achieved with the cut  $-1 < \phi < 1$ , accounting for the insensitivity to the sense. Under these assumptions, the intrinsic neutron-induced background would be  $0.06 \div 0.11$  per year per kilogram.

## 5. Summary

An unambiguous proof of the existence of Dark Matter in the form of WIMP particles would come from the directional observation of induced nuclear recoils. The use of nuclear emulsions both as target and as detector is promising.

One of the most important background for such an experiment comes from proton and nuclear recoils induced by neutrons from the intrinsic radioactive contamination of nuclear emulsions. The trace activity of  $^{238}\text{U}$  and  $^{232}\text{Th}$  radioactive chains have been determined by measuring each nuclear emulsion component by Inductively Coupled Plasma Mass Spectrometry (ICP-MS): the total emulsion activity is 23 mBq  $\text{kg}^{-1}$  for the Uranium chain and 5.1 mBq  $\text{kg}^{-1}$  for the Thorium chain with an uncertainty of 30%. The  $\gamma$ -spectroscopy analysis, performed in order to cross check the results of ICP-MS and to verify the secular equilibrium of the radioactive chains, confirmed the results except for a lower activity of the  $^{226}\text{Ra}$  sub-chain of  $^{238}\text{U}$  for gelatin.

The measured radioactive contaminations have been used to calculate the neutron flux generated by spontaneous fission of  $^{238}\text{U}$  and by  $(\alpha, n)$  reactions with the emulsion elements: it amounts to  $1.2 \pm 0.4$  neutrons per year per kilogram of nuclear emulsion and the energy spectrum has a mean value of about 2 MeV.

A GEANT4 simulation demonstrates that, under certain assumptions on the detector geometry and on the read-out strategy, the detectable neutron-induced background can be reduced down to 0.06 per year per kilogram.

Therefore the neutron-induced background due to the intrinsic radioactive contamination allows the design of an emulsion detector with an exposure of about  $10 \text{ kg} \times \text{year}$ . A careful selection of the emulsion components and a better control of their production could further increase the radiopurity, thus extending the detector exposure.

## Acknowledgments

We warmly thank C. Galbiati and P. Mosteiro for useful discussions on the measurements performed and on the estimate of the neutron background. We are also indebted with V. Kudryavtsev for helps with the SOURCES code. We thank the LNGS chemistry service for the mass spectrometry measurements. We would like to thank K. Oyama of Chemical Instrumentation Facility, Nagoya University, Japan for the measurements of nuclear emulsion composition. This work was also supported by JSPS KAKENHI Grant-in-Aid for Young Scientists (B) Number 25800140 and Grant-in-Aid for Scientific Research on Innovative Areas Number 14429969.

## References

## References

- [1] G. Bertone, D. Hooper and J. Silk, Phys. Rept. **405** (2005) 279.
- [2] V. C. Rubin, N. Thonnard and W. K. Ford, Jr, Astrophys. J. **238** (1980) 471.
- [3] A. K. Drukier, K. Freese, D. N. Spergel, Phys. Rev. D **33** (1986) 3495.
- [4] R. Bernabei et al., Eur. Phys. J. C **73** (2013) 2648.
- [5] D. S. Akerib et al. (LUX Collaboration), Phys. Rev. Lett. **112** (2014) 091303.
- [6] E. Aprile et al. (XENON Collaboration), Phys. Rev. Lett. **109** (2012) 181301.
- [7] G. Angloher et al. (CRESST Collaboration), Eur. Phys. J. C **74** (2014) 3184; G. Angloher et al. (CRESST Collaboration), arXiv:1509.01515 [astro-ph.CO].
- [8] R. Agnese et al. (SuperCDMS Collaboration), Phys. Rev. Lett. **112** (2014) 241302.
- [9] X. Xiao et al., (PandaX Collaboration), Phys. Rev. D **92** (2015) 052004.
- [10] D. N. Spergel, Phys. Rev. D **37** (1988) 1353.
- [11] J.B.R. Battat (DRIFT Collaboration), Phys. Dark Univ. **9-10** (2015) 1-7.
- [12] K. Miuchi et al., Phys. Lett. B **686** (2010) 11.
- [13] S. Ahlen et al., Phys. Lett. B **695** (2011) 124.
- [14] J. Billard et al., J. Phys. Conf. Ser. **309** (2011) 012015.
- [15] A. Alexandrov et al., JINST **9** (2014) C12053.
- [16] T. Katsuragawa et al., J. Phys. Conf. Ser. **469** (2013) 012004.
- [17] T. Nakamura et al., Nucl. Instrum. Meth. A **556** (2006) 80.
- [18] M. Natsume et al., Nucl. Instrum. Meth. A **575** (2007) 439.
- [19] T. Naka et al., Nucl. Instrum. Meth. A **718** (2013) 519.
- [20] K. I. Nagao and T. Naka, Prog. Theor. Exp. Phys. (2012) 043B02.

- [21] K. Morishima and T. Nakano, JINST **5** (2010) P04011;  
N. Armenise et al., Nucl. Instrum. Meth **A 551** (2005) 261.
- [22] S. Agostinelli et al. (GEANT4 Collaboration), Nucl. Instrum. Meth. **A 506** (2003) 250.
- [23] J. S. Becker, *Inorganic Mass Spectrometry - Principles and Applications* (Wiley, 2007), ISBN 9780470012000.
- [24] G. Heusser, Annu. Rev. Nucl. Part. Sci. **45** (1995) 543.
- [25] M. Laubenstein et al., Appl. Radiat. Isot. **61** (2004) 167.
- [26] J. K. Shultis, R. E. Faw, *Fundamentals of Nuclear Science and Engineering* (CRC press, 2007), p. 141, ISBN 1420051369.
- [27] R. Heaton, H. Lee, P. Skensved and B. C. Robertson, Nucl. Instrum. Meth. **A 276** (1989) 529.
- [28] M.J. Berger, J.S. Coursey, M.A. Zucker and J. Chang, *Stopping-Power and Range Tables for Electrons, Protons, and Helium Ions*, National Institute of Standards and Technology, URL <http://physics.nist.gov/PhysRefData/Star/Text/ASTAR.html>.
- [29] N. Tsoulfanidis, *Measurement and Detection of Radiation* (Taylor & Francis, 1995), p.126, ISBN 1560323175.
- [30] W. B. Wilson et al., *SOURCES 4A: A Code for Calculating ( $\alpha,n$ ), Spontaneous Fission, and Delayed Neutron Sources and Spectra*, LA-13639-MS, Los Alamos (1999).
- [31] J. R. de Laeter et al., Pure Appl. Chem. **75** (2003) 683.
- [32] M. J. Carson et al., Astropart. Phys. **21** (2004) 667;  
R. Lemrani et al., Nucl. Instrum. Meth. **A 560** (2006) 454;  
V. Tomasello, V. A. Kudryavtsev and M. Robinson, Nucl. Instrum. Meth **A 595** (2008) 431.